SUPPLEMENTARY INFORMATION

A Nickel Glutamate Metal Biomolecule Framework

Élvio Antônio de Campos*[a], Luana Thayline Casagrande da Silva,[a] Rodrigo Vieira Rodrigues[a], Ronan Farias Freire de Souza[a], Jeane Patrícia Cardozo dos Santos[a], Conceição de Fátima Alves Olguin[a], Cleide Viviane Buzanello[a], Javier Alcides Ellena[b], Pedro Henrique de Oliveira Santiago[b], Sílvia Denofre de Campos[a].

*elvioantonio@uol.com.br

[a] – *Center of Engineering and Exacts Sciences, Unioeste – Western Paraná State University, Campus Toledo, Guaíra Street 3141, ZIP Code* 85903-220*, Toledo, PR, Brazil.*
[b] - *São Carlos Institute of Physics, USP – University of São Paulo, Av. Trab. São Carlense, 400, ZIP Code 13566-590, São Carlos – SP, Brazil.*

Characterization of the Compound I – $[Ni(HGlu)_2]$

FTIR Spectroscopy

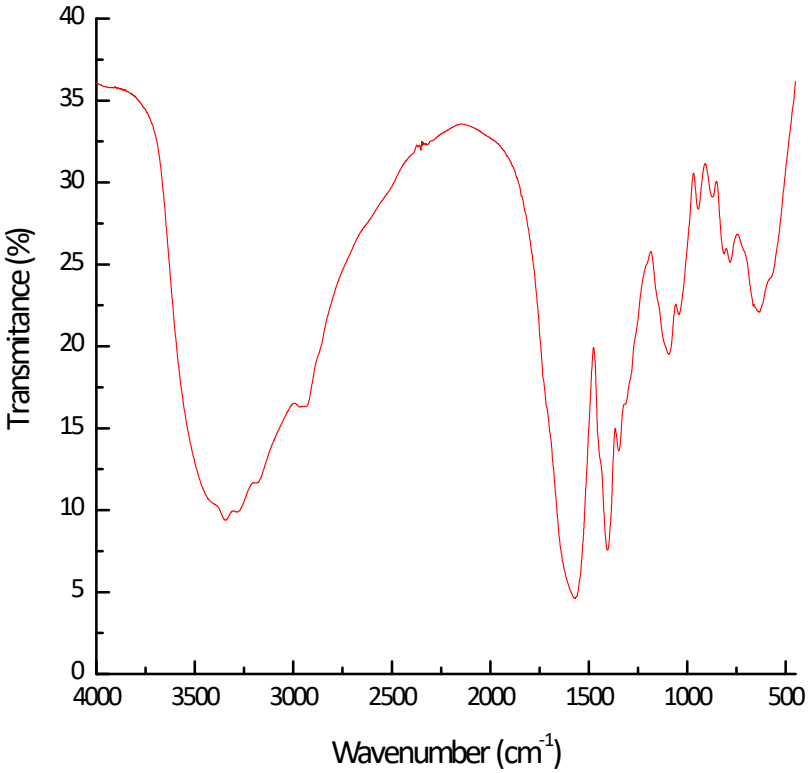

Figure S1: FTIR spectrum of the $[Ni(HGlu)_2]$ in KBr pellets.

The infrared spectrum of the $[Ni(Hglu)_2]$ complex, FIG. S1, shows a broad, intense band between 3600 and 3100 cm^{-1}, probably due to the stretching vibrations of the O-H bonds of the carboxyl group in the amino acid side chain. In this same region there are two bands that stand out from the contours of this

intense band, with maxima at 3344 cm^{-1} and 3284 cm^{-1} (shoulder) and are probably due, respectively, to the asymmetric and symmetric stretching vibrations of the N-H bonds of -NH_2 groups, in this case coordinated to the metal ion. Two other bands stand out in this spectrum: an intense, broad band between 1760 cm^{-1} and 1480 cm^{-1} and a narrow but intense band at 1406 cm^{-1}. The first is probably due to the superimposition of distinct C=O bond stretching bands (coordinated or not) with N-H bond stretching and deformation vibrations of coordinated -NH_2 groups, as well as asymmetric stretching vibrations of coordinated carboxylate groups. The second band (at 1406 cm^{-1}) is probably due to the symmetrical stretching vibrations of -COO^- groups. In the Table S1 are summarised the bands observed in the infrared spectrum of $[Ni(Hglu)_2]$ and their respective assignments [1, 2].

Tab. S1: Selected infrared absorption bands of glutamic acid, the complex $[Ni(Hglu)_2]$ and $\{[Ni(Glu)(H_2O)]\cdot H_2O\}_n$, and their respective assignments.

Attribution	Glutamic Acid	cm^{-1} $[Ni(Hglu)_2]$	$\{[Ni(Glu)(H_2O)]\cdot H_2O\}_n$
ν(-OH) carboxilic acid	3440	3600-3100	-
ν(-OH) H_2O	-	-	3600-3000
$\nu_a(NH_2)$	-	3344	3326
$\nu_s(NH_2)$	-	3284	3248
$\nu_s(NH_3^+)$	3060	-	-
$\nu_s(CH_2)$ carbon sp^3	2965	2990-2900	2961
$\nu_a(CH_2)$ carbon sp^3	2930	2990-2900	2919
ν_s(C=O)	1639	<1760	1615
$\delta(NH_3^+)$	1615 (shoulder)	-	1585 $\delta(NH_2)$ coord.
$\nu_a(COO^-)$	1513	1760-1480	1549
$\delta(CH_2)$ *scissoring*	1436	-	-
$\nu_s(COO^-)$	1417	1406	1419
$\delta(CH_2)$ *wagging*	1387	-	-
δ(CH)	1355 and 1253	-	-
δ(OH)	1311	-	-
$\delta(CH_2)$ *twisting*	1229 and 1210	-	-
$\delta(NH_3^+)$ *rocking*	1147 and 1123	-	-
ν(C-O)	1094	-	-
ν(C-N)	1056	-	-
ν(M-O)	-	-	587
ν(M-N)	-	-	466

Thermal Analysis (TGA/DTA)

Figure S2 shows the mass loss (TGA) and heat flow (DTA) curves as a result of heating the $[Ni(Hglu)_2]$ complex. The TGA curve (blue) shows two main thermal events: a slight and constant loss of mass between 100 and 300 ºC

(approximately 10% of the total mass) and a more obvious loss of mass between 350 ºC and 400 ºC (approximately 60% of the total mass), which is related to the thermal degradation of the organic matter present in the material.

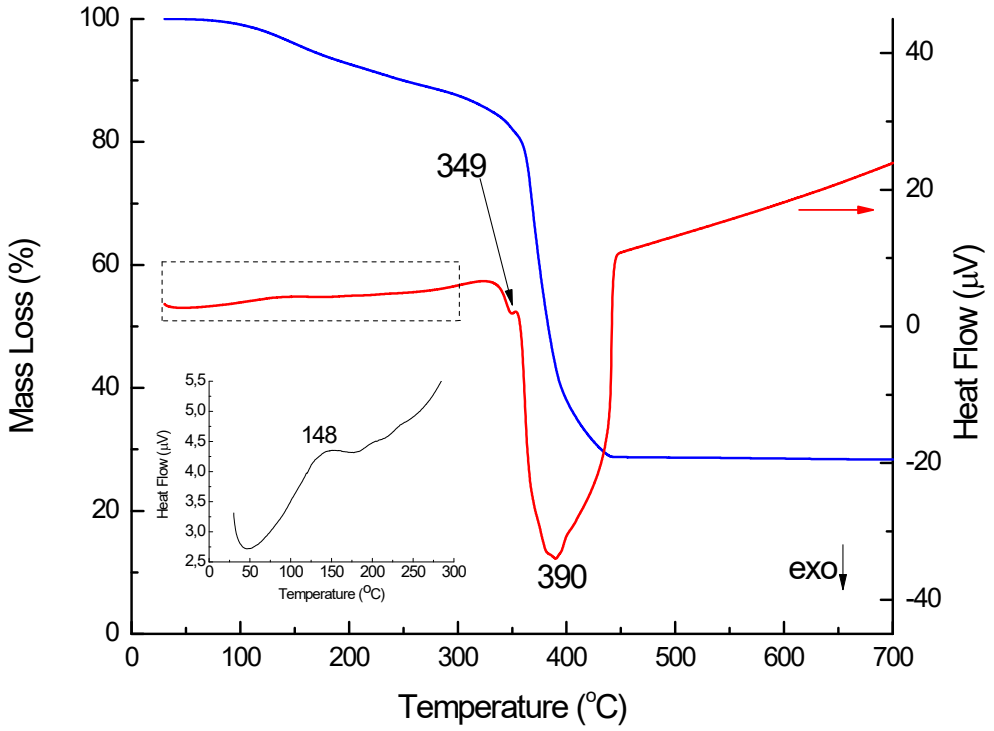

Figure S2: Thermogravimetric curves of the [Ni(Hglu)$_2$] complex: TGA in blue and DTA in red. Inserted graph shows the variation in heat flow as a function of temperature by expanding the y-scale between 2.5 and 5.5 μV).

The DTA curve shows that the degradation stage between 300 and 400 ºC is made up of different thermal events, as in addition to the large and intense exothermic peak, with a maximum very close to 390 ºC, there is a weakly exothermic peak at approximately 349 ºC and an unresolved peak (shoulder) below 450 ºC. The loss of mass between 100 and 300 ºC, on the other hand, occurs with little heat consumption, as a weakly endothermic peak can be seen between 100 and 170 ºC in the inserted graph in Figure S2. Physically adsorbed water molecules show weakly endothermic peaks in the DTA curve, due to the overcoming of interactions between these molecules and the solid material [3]. After heating above 450 ºC, 28.3 % of the initial mass remains. Therefore, the complex probably decomposes on heating into a mixture of nickel carbonate and nickel oxide (NiO).

UV-Vis Spectroscopy

The electronic spectra of the [Ni(Hglu)$_2$] complex are in Figure S3. Note that the spectra of the complex in solution, obtained by conventional spectroscopy, and of the pure solid, obtained by photoacoustics, show the Ni^{2+} ion in an octahedral environment, since the three characteristic bands of the electronic transitions related to the d8 system in the octahedral field are observed [4]. The respective assignments of these bands can be found in the figure itself and in Table S2.

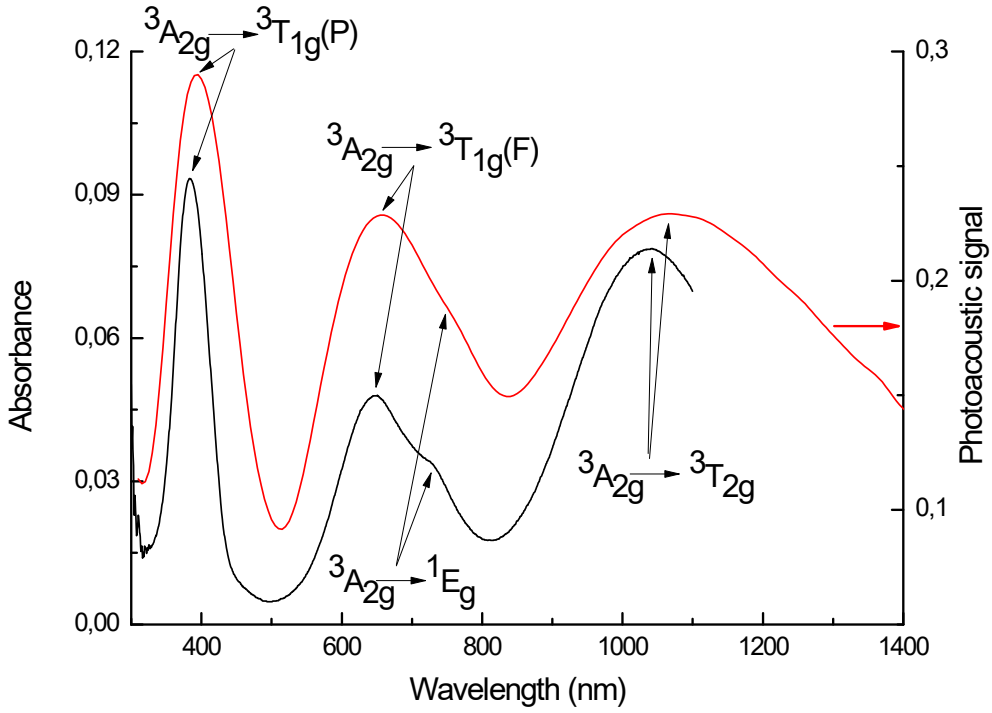

Figure S3: Electronic spectra of the [Ni(Hglu)$_2$] complex and their respective assignments: in black the spectrum of the 10^{-2} mol L^{-1} aqueous solution obtained by conventional absorption spectroscopy and in red the spectrum of the pure solid obtained by photoacoustics.

Tab. S2: Bands observed in the electronic spectra of the [Ni(Hglu)$_2$] complex in solution and in the solid state and their respective assignments.

Transition	Attribution	$\lambda_{máx}$ (nm)	
		solution	solid
ν_1	$^3A_{2g} \rightarrow {}^3T_{2g}$	1038	1067
ν_2	$^3A_{2g} \rightarrow {}^3T_{1g}$ (F)	648	656
ν_2	$^3A_{2g} \rightarrow {}^3T_{1g}$ (P)	384	394

Considering the first transition (ν_1) as 10Dq (Δ_0) we have values of 9634 cm^{-1} for the complex in aqueous solution and 9372 cm^{-1} for the complex in the solid state. This value is slightly higher than the 10Dq value for the $[Ni(H_2O)_6]^{2+}$ complex, which varies between 8230 and 8500 cm^{-1}, and lower than that of the $[Ni(NH_3)_6]^{2+}$ complex, which varies between 10800 and 11053 cm^{-1} [5]. The Racah parameter (B) for nickel complexes can be calculated using Equation 1 [5]:

$$\nu_2 + \nu_3 - 3\nu_1 = 15B \quad (1)$$

Calculating these values from Equation (1), the values observed for the respective transitions in the spectra in Figure S3 and considering that in the isolated Ni^{2+} ion the value of B is 1080 cm^{-1} [5] gives B = 834 cm^{-1} for the complex in solution and B = 838 cm^{-1} for the complex in the solid state. The nefelauxetic ratio β ($B_{compound}$/ $B_{Free\ ion}$) is equal to 0.772 for the complex in solution and 0.779 for the complex in the solid state. For the $[Ni(H_2O)_6]^{2+}$ ion the value of the nefelauxetic ratio is 0.895 and for $[Ni(NH_3)_6]^{2+}$ it is 0.759 [5]. Although these values are very close, the difference in relation to the aquocomplex can be explained by the chelate effect present in $[Ni(Hglu)_2]$, which favours a reduction in electronic repulsion, justifying the lower value of β.

Based on this information, we can suggest that, in solids, coordination is probably carried out by the carboxylic group of the amino acid side chain already coordinated to the metal ion by the carboxyl of the amino acid group. In solution, water molecules probably occupy these sites, shifting the bands to higher energy values, as can be seen in the respective spectrum. In tetrahedral Ni^{2+} compounds, the highest energy band, near 400 nm, is absent [4]. Furthermore, the profile of these spectra is very similar to the spectra of Ni(II) with ligands derived from L-amino acids described in the literature [6].

Mass Spectometry

The mass spectrum obtained for the nickel complex with glutamic acid, Figure S4, shows several peaks of very low intensity, between mass/charge ratios (m/z) of between 100 and 400. The most intense peak is at a mass/charge ratio of 148 and probably corresponds to protonated glutamic acid (M = 148.13 g mol^{-1}). The probable molecular ion peak is at the m/z ratio of 351, with intensity

close to 10 %. This corresponds to the molecular formula where the Ni^{2+} ion is bound to two hydrogen glutamate ions, with a unit charge, which would correspond to the formula $[Ni(HGlu)_2]$ for the reaction product between glutamic acid and basic nickel carbonate. If there were two water molecules in the coordination sphere of the metal ion, the molecular ion peak should appear at m/z close to 387. The different peaks in the mass spectrum in Figure S4 are explained by the fragments proposed in Figure S5 from the complex with an m/z ratio of 351.

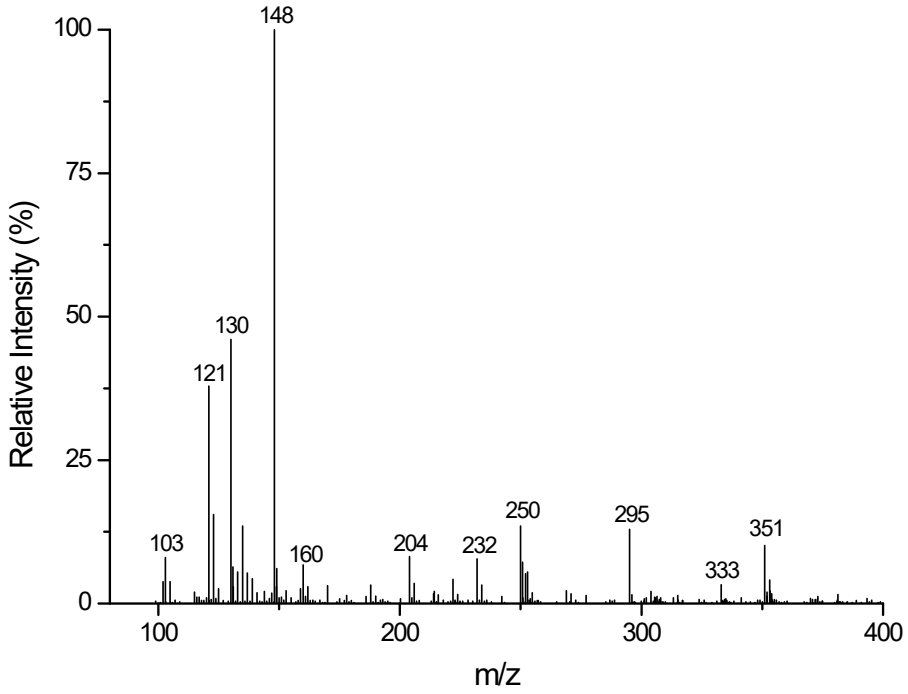

Figure S4: Mass spectrum of the nickel complex obtained by the reaction between basic nickel carbonate and glutamic acid.

Thus, the loss of a water molecule by the $[Ni(HGlu)_2]$ complex leads to the formation of the structure responsible for the peak at m/z of 333. The loss of a -C-COO^- fragment produces the ion with an m/z of 295, just as the loss of the -C-COO^- and -COOH fragments would lead to the ion with an m/z of 250. The loss of a carboxylate ligand corresponds to the formation of the ion with an m/z of 204, while the loss of a glutamate ligand together with the -COO fragment results in the ion with an m/z of 160.

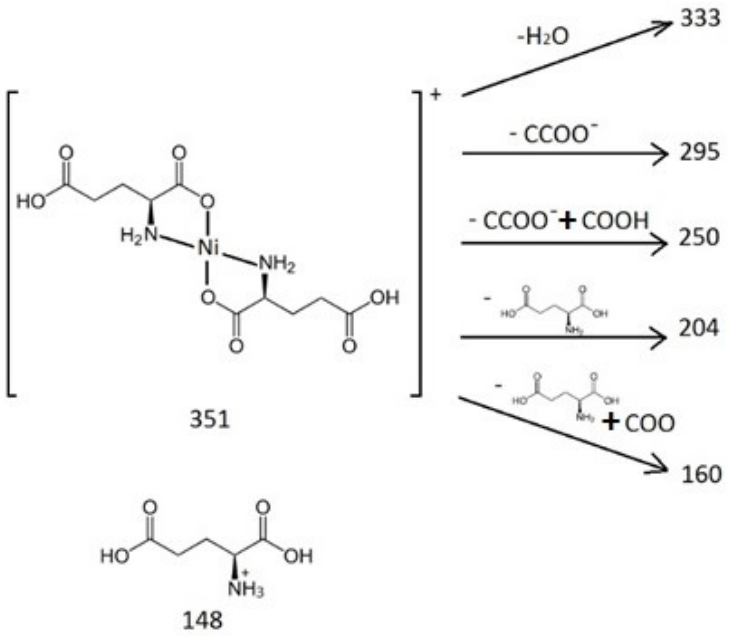

Figure S5: Representation of the loss of fragments of the nickel complex obtained by the reaction between basic nickel carbonate and glutamic acid based on the mass spectrum in Fig. S4.

These decomposition products are similar to those proposed for the decomposition of nickel and manganese complexes with aspartic acid [7].

This information suggests that the molecular formula of the nickel complex obtained is $[Ni(HGlu)_2]$, but with an octahedral coordination environment, which agrees with the elemental analysis, UV-Vis spectroscopy and thermal analyses. To this end, the octahedral coordination environment would be completed by interactions with the carboxyls of the amino acid side chain, through weak interactions.

Characterization of the Compound II – $\{[Ni(Glu)(H_2O)]\cdot H_2O\}_n$

FTIR Spectroscopy

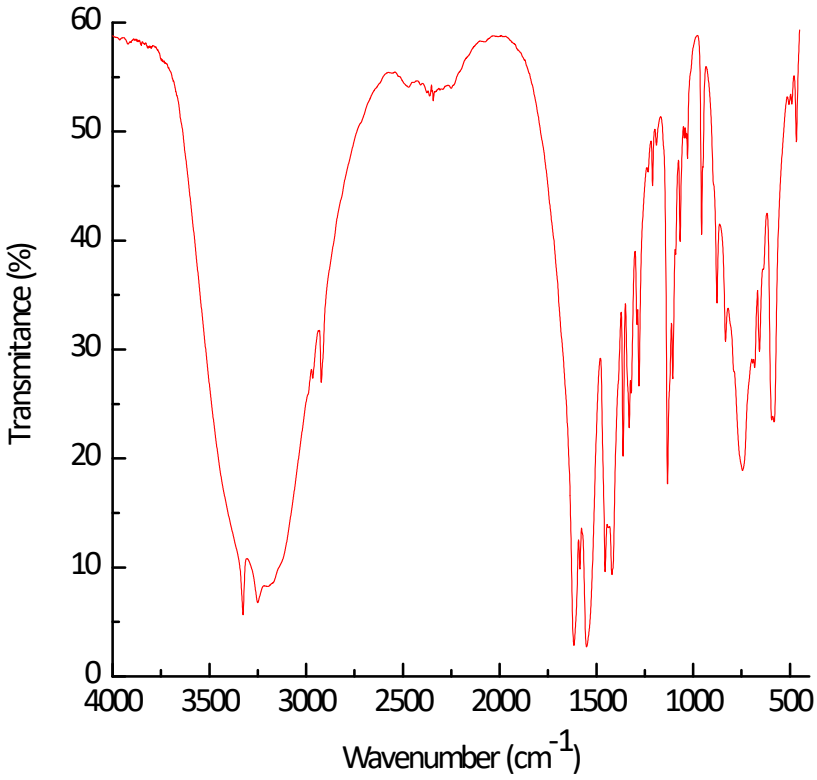

Figure S6: FTIR spectrum of the $\{[Ni(Glu)(H_2O)]\cdot H_2O\}_n$ in KBr pellets.

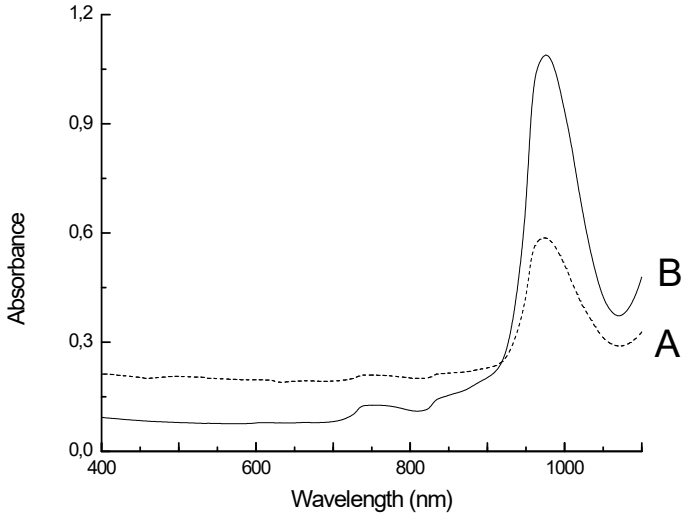

Figure S7: UV-Vis spectra of the **(A)** aqueous solution obtained after washing $\{[Ni(Glu)(H_2O)]\cdot H_2O\}_n$ freshly prepared and **(B)** aqueous solution of the pure glutamic acid.

Microbiological tests

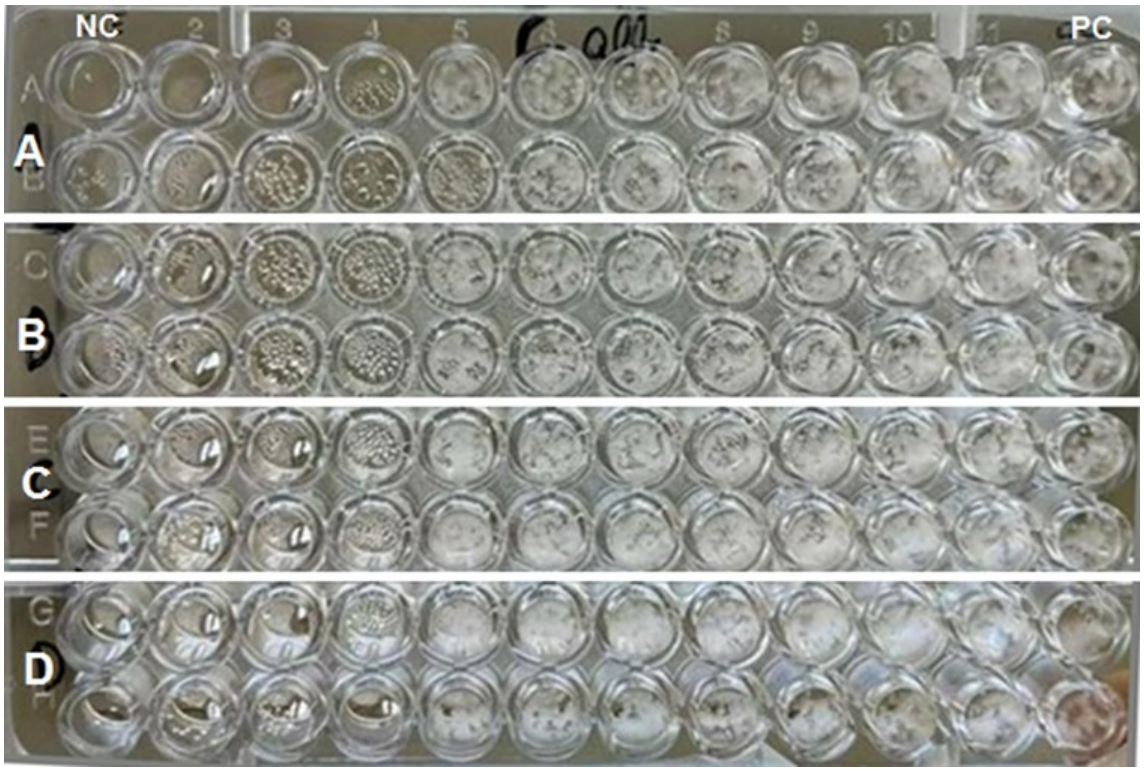

Figure S8: Microdilution plates for *C. albicans* after 24 h of incubation. **A** and **B** = $\{[Ni(Glu)(H_2O)]\cdot H_2O\}_n$; **C** and **D** = $[Ni(HGlu)_2]$; **NC** = negative control; **PC** = positive control.

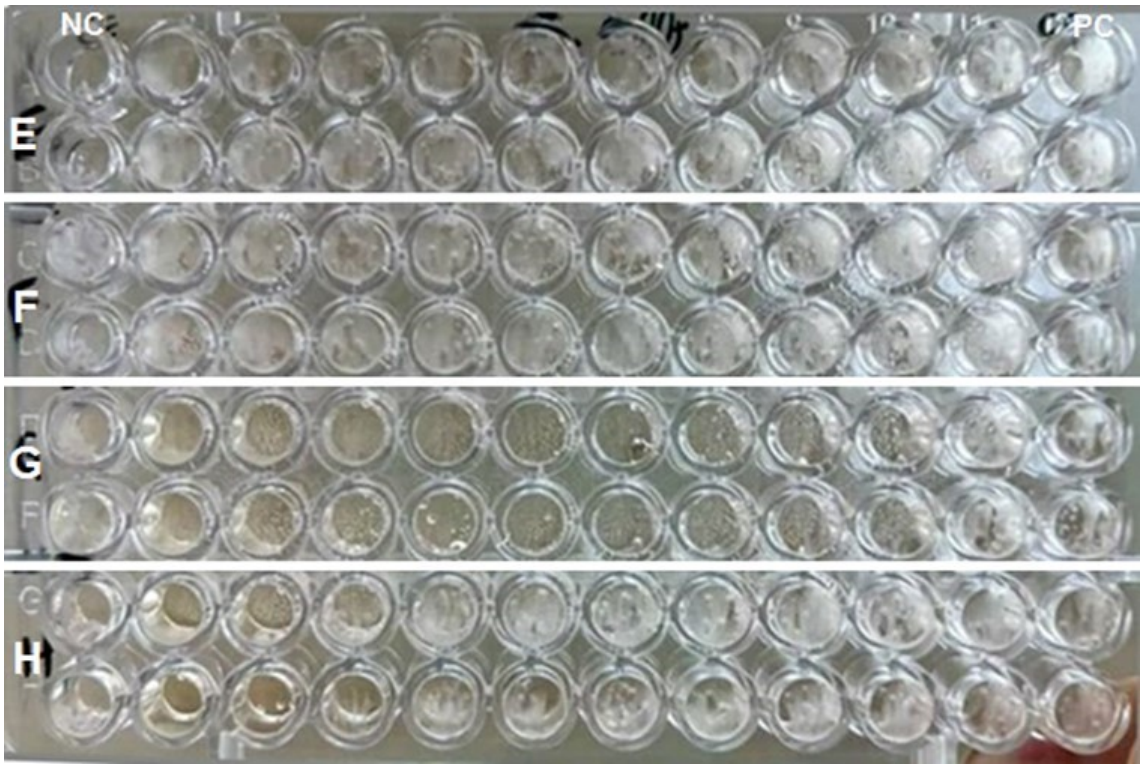

Figure S9: Microdilution plates for *C. albicans* after 24 h of incubation. **E** = glutamic acid; **F** = nickel precursor (basic nickel carbonate); **G** = Fluconazol; **H** = Amphotericin B; **NC** = negative control; **PC** = positive control.

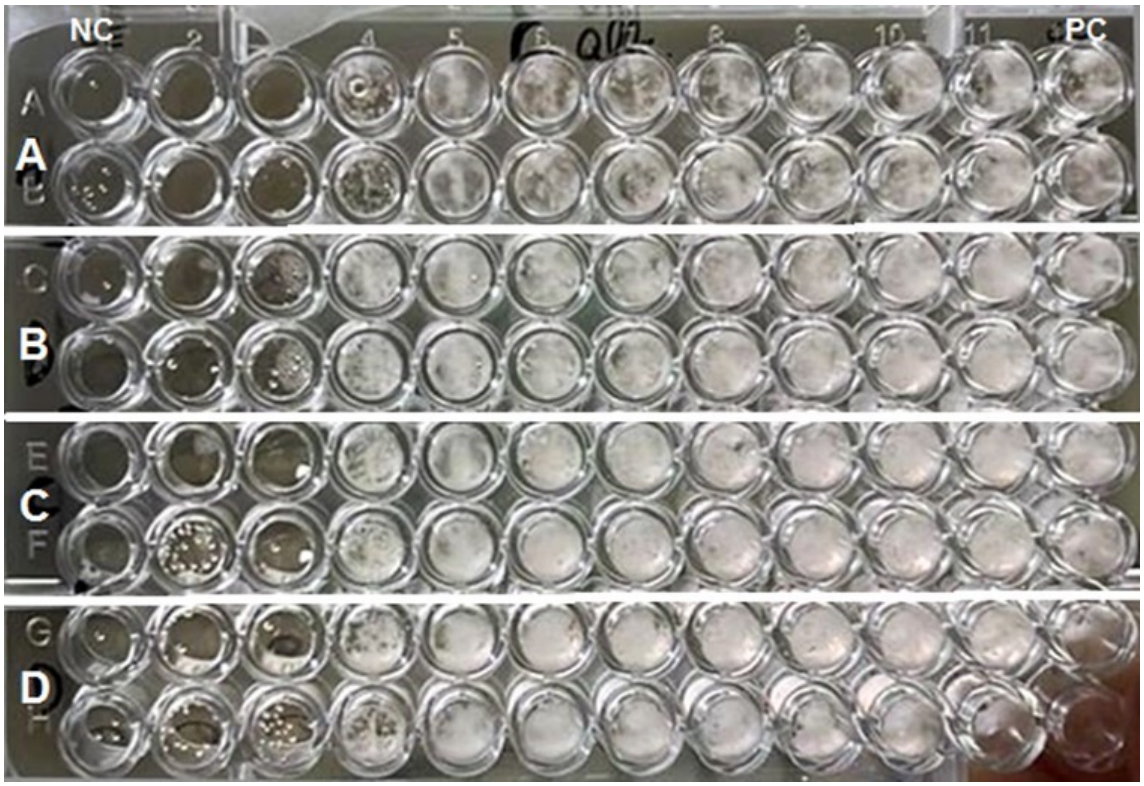

Figure S10: Microdilution plates for *C. albicans* after 48 h of incubation. **A** and **B** = $\{[Ni(Glu)(H_2O)]\cdot H_2O\}_n$; **C** and **D** = $[Ni(HGlu)_2]$; **NC** = negative control; **PC** = positive control.

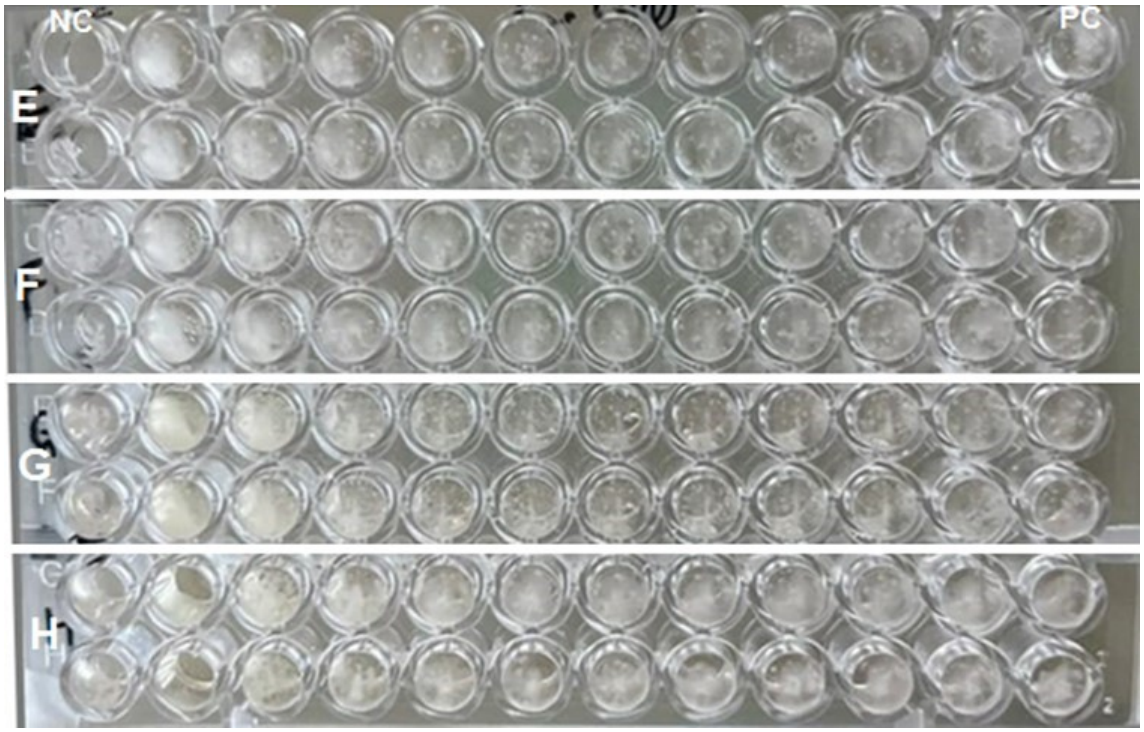

Figure S11: Microdilution plates for *C. albicans* after 48 h of incubation. **E** = glutamic acid; **F** = nickel precursor (basic nickel carbonate); **G** = Fluconazol; **H** = Amphotericin B; **NC** = negative control; **PC** = positive control.

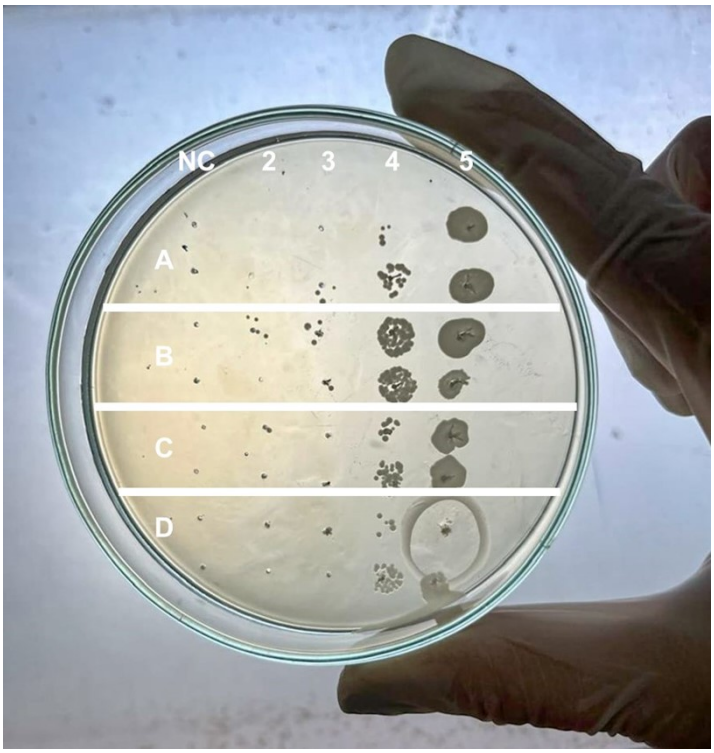

Figure S12: Sub-cultivation plates to *C. albicans* after 48 h of incubation. **A** and **B** = $\{[Ni(Glu)(H_2O)]\cdot H_2O\}_n$; **C** and **D** = $[Ni(HGlu)_2]$; **NC** = negative control; **2–5** = Compounds concentration at 256, 128, 64 and 32 μg mL^{-1}, respectively.

Experimental

Microdilution plates preparation

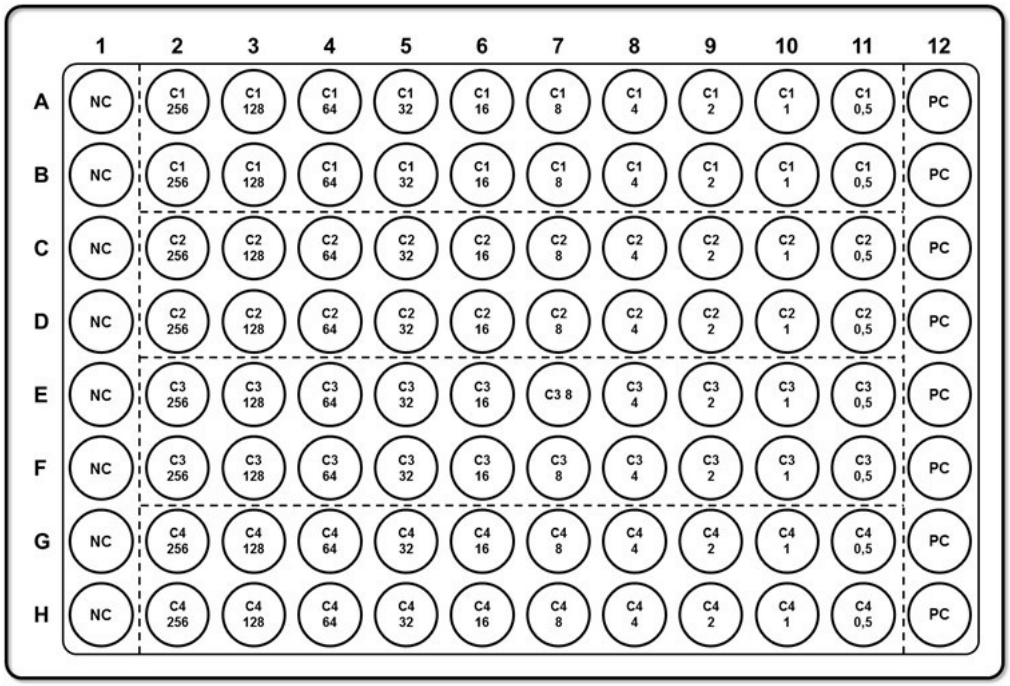

Figure S13: Scheme adopted for the microdilution plates in the MIC tests. **C1–C4** = Tested sample and its concentration in μg mL^{-1}; **NC** = negative control; **PC** = positive control.

Culture medium for Drosophila melanogaster

Figure S14: Images of *Drosophila melanogaster* cultivation.

Toxicity tests for larvae and flies

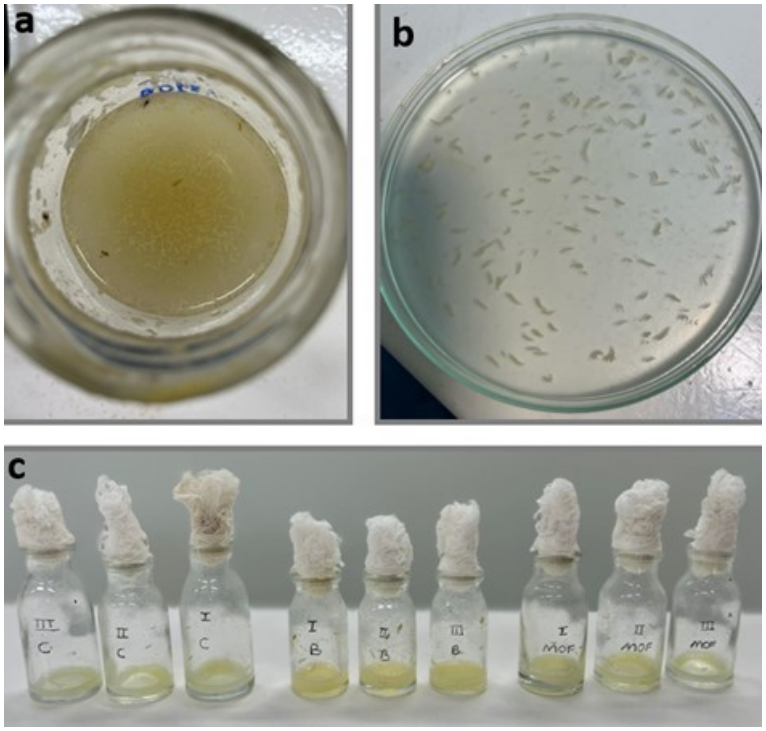

Figure S15: Images of the stages of the toxicity test with *Drosophila melanogaster* larvae. **(a)** Larvae in 10% aqueous sucrose solution; **(b)** Larvae washed with distilled water; **(c)** Toxicity test vials to **(B)** control and (C and MOF) samples.

Figure S16: Images of the stages of the toxicity test with *Drosophila melanogaster* flies. On the left, flies kept without diet for 6 hours. On the right, flies in the vials of the (B) control and (C, M) samples.

References

[1] Dhamelincourt, P.; Ramirez, F. G. JOURNAL OF RAMAN SPECTROSCOPY. 1991; 22:577-582.

[2] Ferenc, W.; Osypiuk, D; Sarzyński, J. et al. ECLÉTICA QUÍMICA. 2020; 45:12−27.

[3] Qiusheng, Z.; Xiaoyan, L.; Jin, Q. et al. RSC ADVANCES. 2015; 5:2100-2112.

[4] Chiboub-Fellah, A.; Meullemeestre, J.; Spies, C. et al. TRANSITION METAL CHEMISTRY. 1999; 24:135-140.

[5] Guhikem, Y., QUIM. NOVA, 2005; 28(1):153-156.

[6] Marquina, A. R.; Movilla, F.; Montilva, O. S. et al. ACTA CRYSTALLOGRAPHICA SECTION B: Structural Science, Crystal Engineering and Materials. 2020; 76:825-838.

[7] Aiyelabola, T. O.; Isabirye, D. A.; Akinkunmi, E. O. et al. JOURNAL OF CHEMISTRY. 2016; 12:1-8.